Available online at www.sciencedirect.com
SCIENCE DIRECT®
Journal of Magnetic Resonance 175 (2005) 1–10
JMR Journal of Magnetic Resonance
www.elsevier.com/locate/jmr

NMR spectroscopy in inhomogeneous B_0 and B_1 fields with non-linear correlation

Daniel Topgaard *, Dimitris Sakellariou [1], Alexander Pines

Materials Sciences Division, Ernest Orlando Lawrence Berkeley National Laboratory and Department of Chemistry, University of California, Berkeley, CA 94720, USA

Received 14 December 2004; revised 4 March 2005
Available online 5 April 2005

Abstract

Resolved NMR spectra from samples in inhomogeneous B_0 and B_1 fields can be obtained with the so-called "ex situ" methodology, employing a train of composite or adiabatic z-rotation RF pulses to periodically refocus the inhomogeneous broadening during the detection of the time-domain signal. Earlier schemes relied on a linear correlation between the inhomogeneous B_0 and B_1 fields. Here the pulse length, bandwidth, and amplitude of the adiabatic pulses of the hyperbolic secant type are adjusted to improve the refocusing for a setup with non-linear correlation. The field correlation is measured using a two-dimensional nutation experiment augmented with a third dimension with varying RF carrier frequency accounting for off-resonance effects. The pulse optimization is performed with a computer algorithm using the experimentally determined field correlation and a standard adiabatic z-rotation pulse as a starting point for the iterative optimization procedure. The shape of the z-rotation RF pulse is manipulated to provide refocusing for the conditions given by the sample-, magnet-, and RF-coil geometry.

Keywords: Inhomogeneous magnetic fields; Chemical shift; Numerical optimization; Adiabatic pulses; z-rotation

1. Introduction

Over the years several methods have been proposed to obtain high-resolution NMR spectra in inhomogeneous magnetic fields. This research is motivated by the possibility to perform high-resolution NMR experiments using cheaper, non-perfect, magnets or intrinsically inhomogeneous designs such as inside-out or single-sided magnets [1,2] that have the potential to dramatically increase the range of situations where NMR can be used.

One class of methods is based on zero- or multiple quantum coherences which evolve under the influence of parameters such as chemical shift and scalar couplings, but independently of the Zeeman interaction, yielding high-resolution information in the indirect dimension [3–7]. This approach is inherently two-dimensional since the signal has to be transformed to single quantum coherences for detection.

A conceptually different approach allows for the detection of a high-resolution spectrum in a single shot [8]. Between each detected point in the FID, z-rotation RF pulses are applied in order to precisely counteract the phase dispersion originating from the inhomogeneous static field B_0 while retaining the modulation due to the chemical shift. This is in contrast to the standard CPMG pulse train that refocuses both the effects of the field inhomogeneity and the chemical shift. Because the detected signal behaves in a way similar to the FID

* Corresponding author. Present address: Physical Chemistry 1, Lund University, P.O. Box 124, SE-221 00 Lund, Sweden. Fax: +46 46 222 4413.
E-mail address: daniel.topgaard@fkem1.lu.se (D. Topgaard).
[1] Present address: DSM/DRECAM/Service de Chimie Moléculaire, CEA Saclay, 91191 Gif-sur-Yvette Cedex, France.

1090-7807/$ - see front matter © 2005 Elsevier Inc. All rights reserved.
doi:10.1016/j.jmr.2005.03.006

obtained in a homogeneous field, incorporation of the detection method in multidimensional techniques is fairly straightforward [9,10].

Very recently, it was demonstrated that the ultra-fast 2D NMR technique developed by Frydman and coworkers [11–13] can be used to obtain resolved NMR spectra in inhomogeneous static fields [14]. Applied static field gradients and selective RF pulses excite the sample slice by slice. The excitation pulses give rise to a phase shift, which is adjusted to cancel the effect of the static field inhomogeneity at the time of signal acquisition.

The key issue for the performance of the z-rotation technique is the ability of the RF pulses to exactly refocus the phase dispersion induced by the static field inhomogeneity ΔB_0. The degree of rotation depends in a controlled way on the magnitude of the RF field B_1. Through spatial matching of ΔB_0 and B_1, conditions can be achieved where the RF pulse z-rotation is opposed by free evolution in the inhomogeneous static field producing nutation echoes [15,16]. A FID-like signal is obtained by repeating the z-rotation pulse and the free evolution period while recording the nutation echo maxima through stroboscopic acquisition.

The ideal refocusing z-rotation pulse is short, in order to minimize the influence of relaxation, diffusion, and direct or indirect coupling evolution, while being capable to control spins over a large bandwidth using a minimum amount of RF power. The composite pulses by Sakellariou et al. [17] have the benefit of being short but have a limited bandwidth defined by the amplitude of B_1. The adiabatic double passage by Meriles et al. [18] is effective over large bandwidths but tends to be rather lengthy. Both these types of pulses are designed for use with linearly correlated ΔB_0 and B_1. The possibility of modifying the adiabatic double passage to provide refocusing even for non-linear profiles was demonstrated with calculations in [19].

Schematic ΔB_0–B_1 correlation functions are shown in Fig. 1. Standard high-field NMR experiments are ideally performed under the conditions shown in (A) with very narrow correlation in both the ΔB_0 and B_1 dimensions. Case (B) with a narrow linear correlation corresponds to the conditions for which the standard z-rotation pulses are effective. Fig. 1D shows in a schematic way the correlation for a single-sided equipment with some, but very broad, correlation. Designing equipment with perfectly linear correlation might be too difficult, but a non-linear correlation as shown in Fig. 1C is not unreasonable. Hence, designing z-rotation pulses for non-linear correlation is an important step towards the realization of true outside-the-magnet "ex situ" NMR spectroscopy.

Tuning of the parameters of the adiabatic pulses has been proposed as a means to provide refocusing even when the correlation between the fields is non-linear

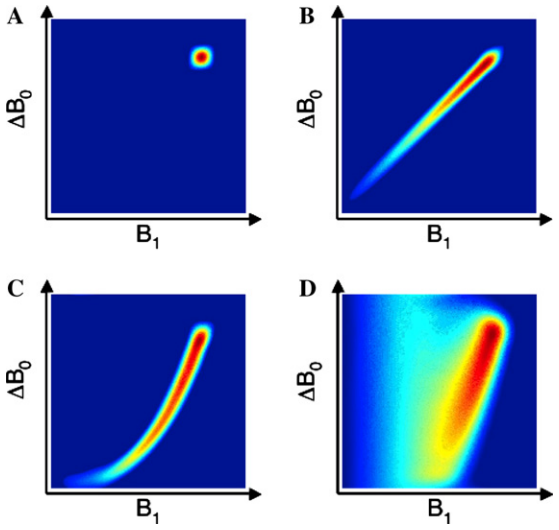

Fig. 1. Schematic ΔB_0–B_1 field correlation functions: (A) homogeneous fields, (B) linear correlation, (C) non-linear correlation, (D) "realistic" correlation for a single-sided system.

[18,19]. Tailoring adiabatic pulses for population inversion over large bandwidths and with great insensitivity to RF inhomogeneity has a long tradition [20–23]. In some sense this kind of optimization is rather straightforward since the pulses induce a transformation between well-defined initial and final states (turning the magnetization from $+z$ to $-z$). More complex is the problem of designing composite or adiabatic constant rotation pulses [23–25], which aim at rotating the magnetization through a specific angle independent of the initial position, RF magnitude, and frequency offset. In the present case, we wish to design a pulse that imposes a z-rotation of the magnetization independent of the initial and final states, but where the amount of rotation depends in a controlled and variable way on the magnitude of B_0 and B_1, thus increasing the complexity of adiabatic pulse design one step further.

Here, we demonstrate a methodology to experimentally determine the correlation between the B_0 and B_1 fields, and then modify an adiabatic z-rotation pulse to improve the refocusing for the conditions given by the sample-, magnet-, and RF-coil geometry.

2. Method

2.1. Spin-1/2 dynamics

An ensemble of non-interacting spin-1/2 nuclei with magnetogyric ratio γ in a static magnetic field $\mathbf{B}_0$ can be described with the magnetization vector $\mathbf{m}$ with Cartesian components m_x, m_y, and m_z. $\mathbf{m}$ is manipulated with an RF magnetic field $\mathbf{B}_1$ oscillating with the frequency ω_{RF} in a plane perpendicular to $\mathbf{B}_0$. The Larmor frequency ω_0 and frequency-offset $\Delta\omega_0$ are defined through

$$\omega_0 = -\gamma B_0, \tag{1}$$

$$\Delta\omega_0 = \omega_0 - \omega_{\mathrm{RF}}, \tag{2}$$

and

$$\omega_1 = -\gamma B_1, \tag{3}$$

quantifies the RF amplitude. The nutation frequency Ω is given by

$$\Omega = \sqrt{\Delta\omega_0^2 + \omega_1^2}. \tag{4}$$

The transformation of the magnetization vector with time t can be written as

$$\mathbf{m}(t) = \mathbf{\Lambda}\mathbf{m}(0), \tag{5}$$

where $\mathbf{\Lambda}$ is a 3×3 rotation matrix. Free precession yields

$$\mathbf{\Lambda} = \begin{pmatrix} \Lambda_{xx} & \Lambda_{xy} & \Lambda_{xz} \\ \Lambda_{yx} & \Lambda_{yy} & \Lambda_{yz} \\ \Lambda_{zx} & \Lambda_{zy} & \Lambda_{zz} \end{pmatrix} = \begin{pmatrix} \cos(\Delta\omega_0 t) & -\sin(\Delta\omega_0 t) & 0 \\ \sin(\Delta\omega_0 t) & \cos(\Delta\omega_0 t) & 0 \\ 0 & 0 & 1 \end{pmatrix} \tag{6}$$

in a frame rotating with frequency ω_{RF} around z. The evolution during an RF pulse of length t_{p} and phase ϕ is given by [26]

$$\begin{aligned}
\Lambda_{xx} &= \frac{(\Delta\omega_0^2 + \Omega^2)\cos(\Omega t_{\mathrm{p}}) + \omega_1^2\{1 + [1 - \cos(\Omega t_{\mathrm{p}})]\cos(2\phi)\}}{2\Omega^2}, \\
\Lambda_{yy} &= \frac{(\Delta\omega_0^2 + \Omega^2)\cos(\Omega t_{\mathrm{p}}) + \omega_1^2\{1 - [1 - \cos(\Omega t_{\mathrm{p}})]\cos(2\phi)\}}{2\Omega^2}, \\
\Lambda_{zz} &= \frac{\Delta\omega_0^2 + \omega_1^2\cos(\Omega t_{\mathrm{p}})}{\Omega^2}, \\
\Lambda_{xy} &= \frac{\omega_1^2[1 - \cos(\Omega t_{\mathrm{p}})]\sin(2\phi)}{2\Omega^2} - \frac{\Delta\omega_0\sin(\Omega t_{\mathrm{p}})}{\Omega}, \\
\Lambda_{yx} &= \frac{\omega_1^2[1 - \cos(\Omega t_{\mathrm{p}})]\sin(2\phi)}{2\Omega^2} + \frac{\Delta\omega_0\sin(\Omega t_{\mathrm{p}})}{\Omega}, \\
\Lambda_{xz} &= \frac{\Delta\omega_0\omega_1[1 - \cos(\Omega t_{\mathrm{p}})]\cos(\phi)}{\Omega^2} + \frac{\omega_1\sin(\Omega t_{\mathrm{p}})\sin(\phi)}{\Omega}, \\
\Lambda_{zx} &= \frac{\Delta\omega_0\omega_1[1 - \cos(\Omega t_{\mathrm{p}})]\cos(\phi)}{\Omega^2} - \frac{\omega_1\sin(\Omega t_{\mathrm{p}})\sin(\phi)}{\Omega}, \\
\Lambda_{yz} &= \frac{\Delta\omega_0\omega_1[1 - \cos(\Omega t_{\mathrm{p}})]\sin(\phi)}{\Omega^2} - \frac{\omega_1\sin(\Omega t_{\mathrm{p}})\cos(\phi)}{\Omega}, \\
\Lambda_{zy} &= \frac{\Delta\omega_0\omega_1[1 - \cos(\Omega t_{\mathrm{p}})]\sin(\phi)}{\Omega^2} + \frac{\omega_1\sin(\Omega t_{\mathrm{p}})\cos(\phi)}{\Omega}.
\end{aligned} \tag{7}$$

The total rotation matrix $\mathbf{\Lambda}_{\mathrm{tot}}$ for any sequence of N RF pulses and free precession periods (neglecting relaxation and diffusion) is given by sequential multiplication from the left of $\mathbf{\Lambda}$ for the individual events:

$$\mathbf{\Lambda}_{\mathrm{tot}} = \prod_{n=1}^{N} \mathbf{\Lambda}_n. \tag{8}$$

2.2. NMR in inhomogeneous fields

The NMR signal from a system with inhomogeneous fields has been treated by, e.g., Hürlimann and Griffin [2]. For such a system the fields defined above depend on position $\mathbf{r}$. Consider a system with spin density $\rho(\mathbf{r})$. The signal $S(t)$ detected by the RF coil can be written as

$$S(t) = \int w(\mathbf{r})\rho(\mathbf{r})s(\mathbf{r}, t)\,\mathrm{d}\mathbf{r}, \tag{9}$$

in which

$$s(\mathbf{r}, t) = m_x(\mathbf{r}, t) + \mathrm{i}m_y(\mathbf{r}, t) \tag{10}$$

and $w(\mathbf{r})$ is a weighting function for the response of the detection system at a given volume element. In the simplest case $w(\mathbf{r})$ is proportional to $B_1(\mathbf{r})$ due to the reciprocity theorem [27]. It could also include information about hardware and software frequency-selective filters or separate excitation and receiver RF coils which may be necessary in order to detect signal only from regions of space where the fields are correlated [19]. In the following we assume that the changes of ω_{RF} are small enough not to affect the values of $w(\mathbf{r})$ appreciably.

In analogy with the treatment by Hürlimann and Griffin [2], Eq. (9) can be recast into

$$S(t) = \iint P(\omega_0, \omega_1)s(\omega_0, \omega_1, t)\,\mathrm{d}\omega_0\,\mathrm{d}\omega_1, \tag{11}$$

where

$$P(\omega_0, \omega_1) = \int w(\mathbf{r})\rho(\mathbf{r})\delta[\omega_0 - \omega_0(\mathbf{r}), \omega_1 - \omega_1(\mathbf{r})]\,\mathrm{d}\mathbf{r} \tag{12}$$

is the field correlation function describing the correlation between the B_0 and B_1 fields weighted with the density of spins and the receiver sensitivity. Here, δ is the two-dimensional Dirac delta-function. For a homogeneous sample $\rho(\mathbf{r})$ is finite and constant within the region of the sample and zero elsewhere. The inclusion of $\rho(\mathbf{r})$ in Eq. (12) implies that only regions containing sample contribute to $P(\omega_0, \omega_1)$. For a system containing species with different chemical shifts $P(\omega_0, \omega_1)$ is convoluted in the ω_0-dimension with the 1D NMR spectrum.

The rationale for the substitution of variables is to remove the explicit space dependence in the expression for the signal. If spin motion can be neglected, the NMR signal can be calculated when $P(\omega_0, \omega_1)$ and the spin response as a function of ω_0 and ω_1 are known. This is achieved without precise knowledge of the spatial variation of the magnetic fields. $P(\omega_0, \omega_1)$ will mostly depend on the magnet and RF-coil design, the sample shape, and to a smaller extent on the electric and magnetic properties of the sample that can distort the fields.

2.3. Determination of the field correlation function

The two-dimensional nutation experiment shown in Fig. 2 has been used to measure resolved NMR spectra in correlated B_0 and B_1 fields [19,28]. Here, we use a

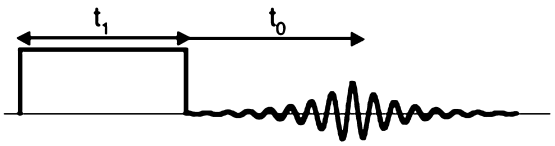

Fig. 2. Pulse sequence for measuring the correlation between the B_0 and B_1 fields. The signal is detected during t_0 under free precession in the B_0 inhomogeneity. A nutation echo is formed if the fields are correlated. The length of the excitation pulse t_1 is incremented in the indirect dimension. A 2D Fourier transform yields a correlation between the offset and nutation frequencies. In a third dimension the carrier frequency ω_{RF} is varied in order to account for off-resonance effects.

similar experiment to obtain an estimate of $P(\omega_0,\omega_1)$ the difference being that the experiment is augmented with a third dimension with varying ω_{RF}.

When off-resonance and finite RF power is taken into account, the signal acquired as a function of the square excitation pulse length t_1 and the free evolution time t_0 is given by

$$S(t_0,t_1)=\iint P(\omega_0,\omega_1)\frac{\omega_1}{\Omega}\left\{\sin(\Omega t_1)+\mathrm{i}\frac{\Delta\omega_0}{\Omega}[1-\cos(\Omega t_1)]\right\}\exp(\mathrm{i}\Delta\omega_0 t_0)\,\mathrm{d}\omega_0\,\mathrm{d}\omega_1. \tag{13}$$

Eq. (13) can be derived by inserting the relevant components of the rotation matrix in Eq. (7) into Eq. (11). One set of $S(t_0,t_1)$ contains all the information about $P(\omega_0,\omega_1)$. In principle, $P(\omega_0,\omega_1)$ could be estimated by assuming a grid of ω_0 and ω_1 values, and then adjust the value of $P(\omega_0,\omega_1)$ at each grid point using some computer algorithm until $S(t_0,t_1)$ calculated with Eq. (13) agrees experiment. A reasonable grid would contain on the order of 100×100 to 1000×1000 grid points and thus the same number of adjustable parameters. In practice it is too computationally demanding to solve Eq. (13) with such a direct approach and it is necessary to reduce the number of unknowns.

Eq. (13) reduces to

$$S(t_0,t_1)=\iint P(\omega_0,\omega_1)\sin(\omega_1 t_1)\exp(\mathrm{i}\Delta\omega_0 t_0)\,\mathrm{d}\omega_0\,\mathrm{d}\omega_1 \tag{14}$$

if off-resonance effects can be neglected, i.e., $\Delta\omega_0 \ll \omega_1$. This is the case if the static field gradient can be turned off during the excitation pulse. Here we assume that the gradients are inherent in the equipment design. Switching of the gradients is thus not a choice.

In the ideal case $P(\omega_0,\omega_1)$ could be determined through a 2D Fourier transform (FT) of $S(t_0,t_1)$. For an experiment where the static field inhomogeneity is on the same scale, or larger, than the maximum RF amplitude, the on-resonance condition is not fulfilled thus prohibiting such a direct approach. A 2D FT is sufficient to extract high-resolution cross-sections or projections [19,28] despite off-resonance artifacts. For a band of frequencies close to resonance the 2D FT also gives quantitative estimates of in what ω_0–ω_1 pairs $P(\omega_0,\omega_1)$ is non-zero. Through a set of nutation experiments with varying ω_{RF} a trace of relevant ω_0–ω_1 pairs can be extracted from the full ω_0–ω_1 space.

Using the proposed method to determine $P(\omega_0,\omega_1)$ is clearly less cumbersome than the spatial mapping of the magnetic fields. A more accurate determination of $P(\omega_0,\omega_1)$, especially when the correlation is not perfect, is a subject that requires, and deserves, further studies. This could be achieved with non-FT methods of data analysis or pulse sequences where the information about ω_1 originates from adiabatic z-rotation pulses [29].

2.4. Pulse optimization

The pulse sequence for high-resolution NMR in inhomogeneous B_0 and B_1 fields is shown in Fig. 3. After an initial excitation pulse, a train of z-rotation RF pulses prevents loss of coherence due to precession in the inhomogeneous static field while preserving the chemical shift modulation. For sufficiently strong RF fields, such as with the composite z-rotation pulses [17], chemical shift evolution takes place only in the delay t_{dw} between adjacent pulses. This is also the case for adiabatic double passages where the chemical shift evolution is effectively refocused at the end of the pulse. For such an ideal case the signal from an ensemble of spins with shift

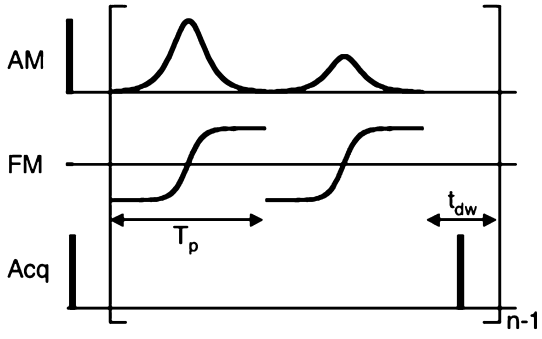

Fig. 3. Pulse sequence for measuring high-resolution NMR spectra in inhomogeneous B_0 and B_1 fields in a single shot. z-rotation RF pulses with amplitude- and frequency-modulation (AM and FM), which counteract the inhomogeneous broadening, are applied between each detected point in the FID. The z-rotation pulses consist of an adiabatic double passage of the hyperbolic secant type [30] where the second passage in each pair has a different amplitude than the first. Each adiabatic full passage can be described with its length T_p, bandwidth, and amplitude. The signal is digitized in the middle of a delay with length t_{dw} between each double passage. As the point of departure for the computer optimization the following parameters were used: amplitude ratio 0.5, bandwidth 5 kHz, $T_p = 1.7$ ms, and $t_{dw} = 0.19$ ms. With $n = 128$ points in the FID the whole sequence takes 460 ms to execute where, to a good approximation, chemical shift evolution takes place during 24.3 ms of these.

δ (expressed in units of rad/s) at the nth point in the FID is given by [17]

$$S(n) = S_0 \exp[in(\delta t_{dw} + \varphi)] \tag{15}$$

neglecting any kind of signal damping. ϕ/t_{dw} is an overall frequency shift independent of δ.

The total rotation matrix for a z-rotation pulse with subsequent free precession delay can be calculated with Eq. (8). The ideal rotation matrix corresponding to Eq. (15) can be formulated as

$$\Lambda(\delta, \Delta\omega_0, \omega_1) = \begin{pmatrix} \cos(\delta t_{dw} + \varphi) & -\sin(\delta t_{dw} + \varphi) & 0 \\ \sin(\delta t_{dw} + \varphi) & \cos(\delta t_{dw} + \varphi) & 0 \\ 0 & 0 & 1 \end{pmatrix}. \tag{16}$$

For a perfect spectrum this rotation matrix should be obtained for all values of $\Delta\omega_0$ and ω_1. If there is no net chemical shift evolution during the z-rotation pulse, the spectral width of the spectrum obtained by FT of the FID is given by $1/t_{dw}$. An adiabatic double passage with unequal amplitude provides a z-rotation that is independent of offset and approximately proportional to B_1 [18]. With unequal pulse length or sweep width the phase shift is no longer proportional to B_1 and in addition depends on the offset [19]. For such a case it is still required that the phase shift θ acquired during a pulse followed by a delay should be unique for each δ, but independent of $\Delta\omega_0$ and ω_1. In addition, the RF pulse should not mix transverse and longitudinal magnetization. The objective function χ^2 for pulse optimization can according to those criteria be defined as

$$\chi^2 = \sum_i \sum_j P_j \lfloor w_1(\theta_{ij}^x - \theta_i^{ideal})^2 + w_1(\theta_{ij}^y - \theta_i^{ideal})^2 + w_2(M_{ij}^x - 1)^2 + w_2(M_{ij}^y - 1)^2 + w_3(M_{ij}^z - 1)^2 \rfloor, \tag{17}$$

where

$$P_j = P(\omega_{0,j}, \omega_{1,j})\, d\omega_{0,j}\, d\omega_{1,j},$$

$$\theta_{ij}^x = \arg[\Lambda_{xx}(\Delta\omega_{0,j}, \omega_{1,j}, \delta_i) + i\Lambda_{yx}(\Delta\omega_{0,j}, \omega_{1,j}, \delta_i)],$$

$$\theta_{ij}^y = \arg[\Lambda_{yy}(\Delta\omega_{0,j}, \omega_{1,j}, \delta_i) - i\Lambda_{xy}(\Delta\omega_{0,j}, \omega_{1,j}, \delta_i)],$$

$$\theta_i^{ideal} = \frac{\sum_j P_j \theta_{ij}^x + \sum_j P_j \theta_{ij}^y}{2\sum_j P_j},$$

$$M_{ij}^x = |\Lambda_{xx}(\Delta\omega_{0,j}, \omega_{1,j}, \delta_i) + i\Lambda_{yx}(\Delta\omega_{0,j}, \omega_{1,j}, \delta_i)|,$$

$$M_{ij}^y = |\Lambda_{yy}(\Delta\omega_{0,j}, \omega_{1,j}, \delta_i) - i\Lambda_{xy}(\Delta\omega_{0,j}, \omega_{1,j}, \delta_i)|,$$

$$M_{ij}^z = \Lambda_{zz}(\Delta\omega_{0,j}, \omega_{1,j}, \delta_i),$$

and w_1, w_2, and w_3 are weighting parameters. This definition of χ^2 is by no means unique, but through extensive simulations it has been found that a smaller value of χ^2 as defined in Eq. (17) corresponds to what among NMR spectroscopists would be perceived as a "better" spectrum. In the general case, the phase shift induced by the adiabatic pulses depends on offset and there is no way to discriminate between offset originating from chemical shift or field inhomogeneity. The objective function in Eq. (17) penalizes pulses with offset dependence under the conditions given by the field correlation and the spectral range of interest. Outside this range there is no control over the effect of the pulse.

The aim of this work is to improve the NMR spectra for samples in inhomogeneous B_0 and B_1 fields correlated in a non-linear way. This corresponds to finding the RF pulse that rotates the transverse magnetization in a way that exactly cancels the phase dispersion originating from the inhomogeneous B_0 field. This must be achieved without affecting the magnitude of either the transverse or longitudinal components of the magnetization. Eq. (17) is the mathematical equivalent of these statements.

3. Experimental

3.1. NMR experiments

Experiments were performed at a proton resonance frequency of 180 MHz using a Varian/Chemagnetics Infinity spectrometer with a super wide-bore magnet. The probe is equipped with an imaging probehead containing three perpendicular gradient coils (x, y, and z) and a conical RF-coil designed for providing a constant B_1 gradient in the x-direction. This setup has been described in detail previously by Sakellariou et al. [17]. A sample located within the coil will experience a linear correlation between the B_0 and B_1 fields when the x-gradient coil is active. A 5 mm OD disposable NMR tube, shortened to a length of 2 cm and filled with a mixture of water and isopropanol, was located as shown in Fig. 4. A steady current was applied to the x-gradient coil yielding a 5 kHz wide peak through direct detection of the FID.

The field correlation function was estimated by a set of 2D nutation experiments as described in paragraph 2.3. One hundred and twenty-eight complex points were digitized in the direct dimension using a dwell time of 50 μs. The length of the excitation pulse was incremented 32 times in steps of 60 μs. In the third dimension the carrier frequency was varied in 10 steps over a range covering 5 kHz. For each point in the 3D data array a single transient was collected using a recycle delay of 2 s. Each 2D dataset $S(t_0, t_1)$ was evaluated by a 2D FT. A single 2D dataset was constructed by collecting slices centered on the carrier frequency from the ten 2D datasets.

Chemical-shift resolved NMR spectra were obtained with the pulse sequence in Fig. 3 employing a square

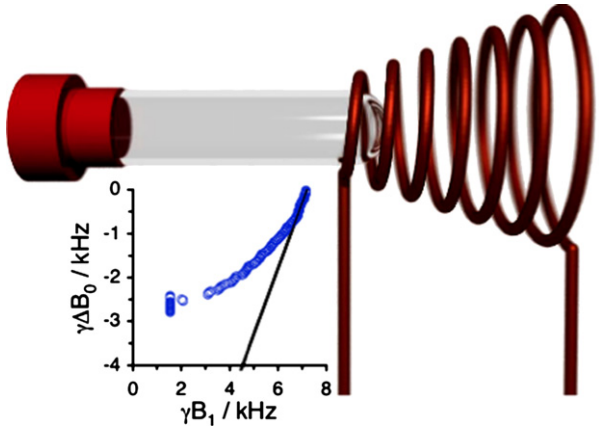

Fig. 4. Sample- and RF-coil geometry together with the experimental ΔB_0 and B_1 field correlation. The 5 mm OD (4 mm ID) sample tube is located just outside the region with maximum B_1, which decays in a non-linear way along the sample. The B_0 gradient is produced using an x-gradient coil (not shown) with dimensions not much larger than the RF-coil. B_0 will thus also vary in a non-linear way along the tube. The blue circles are extracted from the isopropanol ridge in the contour plot in Fig. 5A. The black line symbolizes one of the possible field correlations for which the standard z-rotation pulses are effective.

excitation pulse and adiabatic double passage z-rotation pulses [18]. One hundred and twenty-eight complex data points were digitized, one in the middle of each free precession delay. For each spectrum 64 transients were acquired with a recycle delay of 2 s. The best possible spectrum using the standard adiabatic double passage with hyperbolic secant amplitude- and phase-modulation [30], where the two pulses have identical bandwidth and pulse length but different amplitude, was obtained by manually adjusting the bandwidth, pulse length T_p, carrier frequency ω_{RF}, free precession delay t_{dw}, and length of excitation pulse t_{90}. The best results were obtained for the following parameters: amplitude ratio 0.5, bandwidth 5 kHz, $T_p = 1.7$ ms, $t_{dw} = 0.19$ ms, $t_{90} = 30$ μs, and $-\omega_{RF}/2\pi = 179.972$ MHz.

Through experiments and simulations it was found that it was sufficient to digitize the z-rotation pulse in 200 steps without degrading the pulse performance significantly. The smaller the number of digitization steps, the faster are the computer calculations, and 200 steps were found to be a reasonable compromise between speed and accuracy. The pulse shape was defined with amplitude- and phase-modulation.

3.2. Numerical pulse optimization

The computer optimization of the z-rotation pulse was implemented in Matlab 5.2 using the "constr" function in the Optimization Toolbox. The band of relevant ω_0–ω_1 pairs was estimated as described above. For the optimization 100 pairs were chosen along this band. The value of $P(\omega_0, \omega_1)\mathrm{d}\omega_0\mathrm{d}\omega_1$ for each pair was assumed to be proportional to the magnitude of ω_1 weighted with a Gaussian centered on ω_{RF}. The width of the Gaussian was set to 600 Hz. This weighting mimics the slice selection from the square excitation pulse. With the chosen $P(\omega_0, \omega_1)$ computer optimization of t_{dw} yielded the same value as the one determined by manual optimization of the experimental NMR spectrum using the standard adiabatic pulses.

To cover the chemical shift range of the sample, the optimization was performed for eight components covering the shift range from −1 to 5 ppm as referenced to the isopropanol peak. The shift difference between water and isopropanol is about 3.5 ppm according to experiments in a homogeneous static field.

The optimization of the adiabatic double passage was carried out with six adjustable parameters: the amplitude, bandwidth, and pulse length for each full passage. ω_{RF} and t_{dw} were fixed at the values obtained through manual optimization of the standard pulse at the spectrometer. Using a 900 MHz Apple iBook the optimization took a couple of minutes.

4. Results and discussion

4.1. Field correlation

The experimentally determined correlation between the RF and static magnetic fields $P(\omega_0, \omega_1)$ is shown as a contour plot in Fig. 5A. Two bands corresponding to water (left) and isopropanol (right) are visible. The bands have a considerable curvature and are leveling off at the strongest B_1. It should be noted that the method yields a perfectly linear correlation when the sample is put in the region of the coil where the correlation according to RF- and gradient-coil design is supposed to be linear. A trace of ω_0–ω_1 pairs was obtained by fitting a polynomial to the isopropanol ridge. This trace was subsequently used for computer optimization of the adiabatic double passage.

4.2. Pulse optimization

The phase acquired during a z-rotation pulse and subsequent free precession delay as a function of ω_0 and ω_1 together with the experimentally determined field correlation is shown in Fig. 5. Pictorially, the optimization can be seen as trying to align the lines of equal phase along the ridges of the field correlation. It is worth repeating that the initial pulse for the optimization was determined by simple trial and error at the spectrometer. The lines of equal phase for this pulse follow the field correlation at the same ω_{RF} as the one experimentally determined to give the best spectrum. The phase lines for the optimized pulse follow the field correlation over larger intervals.

From Fig. 5A information about the resulting spectrum can be extracted. The figure shows the phase shift

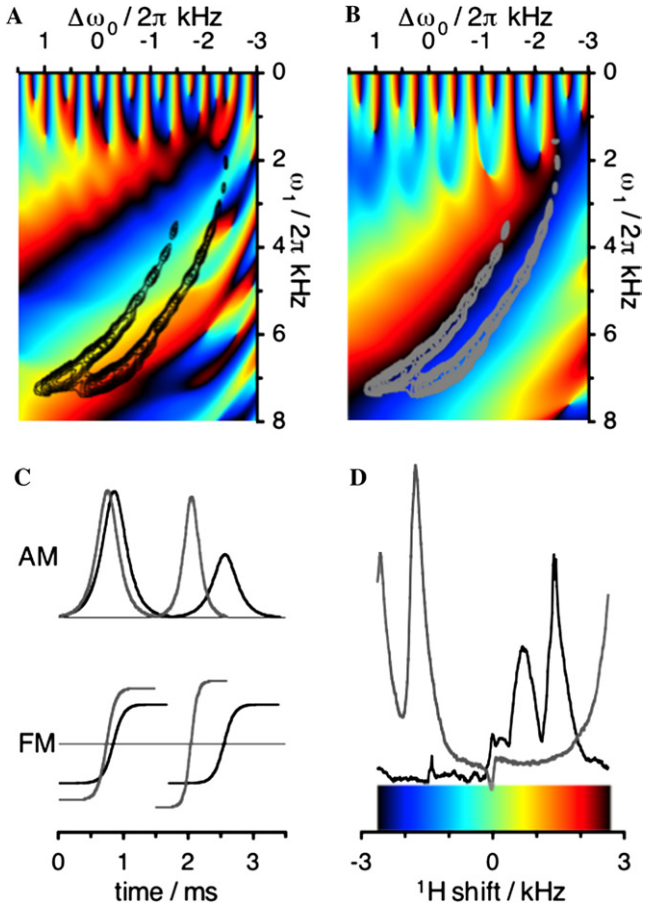

Fig. 5. Results of the field correlation and pulse optimization experiments. The identical contour plots in (A) and (B) show the field correlation $P(\omega_0, \omega_1)$ determined with the experiment in Fig. 2. The two ridges originate from water (left) and isopropanol (right). The standard (black) and optimized (gray) z-rotation pulses and corresponding NMR spectra obtained with the pulse sequence in Fig. 3 are shown in (C) and (D), respectively. The underlying color patterns in (A) and (B) indicate the calculated rotation of the transverse magnetization during an adiabatic double passage followed by a free precession delay for the standard (A) and optimized (B) pulses. The color-coding corresponds to the phase shift between each point in the FID and the position in the final spectrum as shown with the color bar in (D). (For interpretation of the references to color in this figure, the reader is referred to the web version of this paper.)

between each detected point in the FID. The color-coding can be directly translated to position in the spectrum. By following the trace of a specific chemical shift component one can predict the peak position and width in the final spectrum. A perfect correspondence between field correlation and equal phase lines implies that all signal originating from this chemical shift component will add to the same position in the spectrum thus giving a sharp peak. For cases where the field correlation and phase lines coincide over a limited region the signal from a small part of the sample add coherently, giving a peak in the spectrum, while the rest of the signal is spread over the spectrum contributing to the baseline. Broadened peaks will be the result for field correlations and phase lines that almost, but not perfectly, coincide. In terms of spectral resolution it is preferable if the phase lines and field correlation agree perfectly over a limited region and not at all in the other regions.

Figs. 5A and B show the rotation of the transverse magnetization, which does not completely describe what will be found in the spectrum. Mixing of longitudinal and transverse magnetization gives rise to a slowly decaying, non-modulated, signal in the FID, which yields an intense peak in the middle of the spectrum [10]. This peak resembles the quadrature glitch resulting from a DC offset between the real and imaginary channels of the receiver, but the origin is fundamentally different and it cannot be easily removed with phase cycling unless each z-rotation pulse in the refocusing pulse train is cycled independently. Post-acquisition processing of the FID baseline removes this artifact effectively. Such treatment was performed for all the spectra presented here.

The standard and optimized z-rotation pulses are shown in Fig. 5C. The computer changes the adiabatic double passage from two passages with identical frequency modulation and different amplitude to two passages with almost equal magnitude, covering twice as wide bandwidth as the initial pair, and with the second passage occurring faster than the first. Although the pulse shape was implemented with phase modulation on the spectrometer and in the calculations, Fig. 5C shows the equivalent frequency modulation since this representation better visualizes the change during the optimization.

The peak positions in Fig. 5D agree with inspection of the field correlation ridges in Figs. 5A and B. For the initial pulse the lines are located in the region with positive (red) phase shifts corresponding to the right side of the spectrum. The peaks for the optimized pulse are located on the left side of the spectrum, which corresponds to the region with negative (blue) phase shifts in Fig. 5B. Recently, Antonijevic and Wimperis obtained resolved 1D spectra by shearing and projecting 2D correlation spectra [28]. The z-rotation pulses can be considered as performing this non-linear shearing and projection in a single shot. The color coding in Figs. 5A and B shows how the shearing is done.

A comparison between the experimental spectra obtained with the standard and optimized pulses is made in Fig. 6. For facilitating the comparison, the spectra have been frequency shifted in order for the maxima to coincide. The optimized pulse is able to provide an NMR spectrum with increased peak amplitudes. The reason for the improvement needs examination. Although it was not set as a goal for the optimization, the final pulse is somewhat shorter than the standard one. This means that the same effective chemical shift evolution takes place in a shorter time. Relaxation and

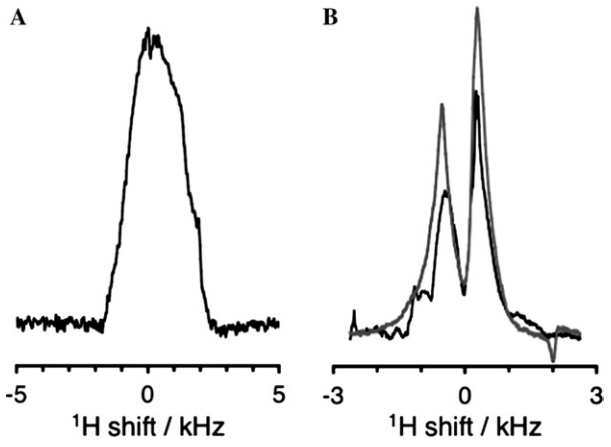

Fig. 6. Experimental spectra for a mixture of water and isopropanol in inhomogeneous fields produced with the setup in Fig. 4. (A) Result of a simple 90-acquire experiment. (B) Obtained with the pulse sequence in Fig. 3 using standard (black) and optimized (gray) z-rotation pulses.

molecular diffusion during the pulse train both act to damp the signal. A shorter pulse means less time for signal damping leading to sharper peaks with the same total area, at least if damping before the first detected point in the FID can be neglected. As is clear from Fig. 6, there is an increase in the peak area for the optimized pulse, implying that this pulse indeed is capable of refocusing spins in a larger part of the sample. The residual line width can mostly be attributed to B_0 inhomogeneity which is not correlated with B_1 and thus cannot be corrected with the current implementation of the ex situ methodology. However, the requirements of perfect field matching could be relaxed with the use of the recently demonstrated ''shim pulse'' methodology [31].

5. Conclusions and outlook

A method was developed for calculating chemical-shift resolved NMR spectra in the presence of inhomogeneous magnetic fields using an experimentally determined correlation between B_1 and B_0. With this method, an objective function for improving spectral quality was defined. These conditions were used in the computer optimization of z-rotation RF pulses yielding improved experimental spectra.

The optimization was demonstrated for an adiabatic double passage using relatively few adjustable parameters. Adapting the technique for a more general pulse optimization using Monte Carlo [22] or optimal control [32] methods is straightforward. These approaches will probably be useful for finding pulses for field correlations with complicated shape where it is unlikely that the perfect pulse can be described with any analytical function. Furthermore, it is also unlikely that hardware optimizations will produce perfectly linearly correlated fields over large sample volumes.

One important simplification during this work was that the spins were assumed to be stationary and experience the same fields throughout the pulse. Just as in MRI [33], there is a diffusion limit to the resolution attainable with this technique. In addition to performing the optimization with the purpose of improving the spectrum, the method could be used for finding pulses that are shorter, and less susceptible to diffusion effects, by including the appropriate penalty function in the definition of the objective function. The diffusion effect merits further studies in order to determine the maximum gradient that is tolerated when designing single-sided magnets for high-resolution experiments. Even if the gradients with currently existing single-sided designs [1] could be handled with the broadband adiabatic pulses, it is presently uncertain if the refocusing effect would be spoiled by spin motion during the pulse. Extension of the work presented here to systems where the spins are allowed to move is clearly feasible.

For maximum signal the performance of the excitation pulse also needs to be taken into account. It is not clear that the pulses designed to be insensitive to large B_0 and B_1 inhomogeneity [24] will be the most effective for the present case with highly correlated B_0 and B_1 fields. For this case it is sufficient that the pulse provides excitation along a well-defined B_0–B_1 band. The optimization technique could be adapted for this purpose using the already existing broadband excitation pulses as a starting point. Additionally, special narrowband [25] pulses could be designed to excite only those spins experiencing correlated fields.

The starting pulse for computer optimization was here first optimized manually at the spectrometer. This tedious work was necessary since the field correlation was not exactly known on account of the approximate analysis using a 2D Fourier transform. With the numerous alternative ways of analyzing 1D and 2D NMR data [34–38] it is reasonable to assume that one of these methods could be adapted to more accurately determine the field correlation. With precise knowledge of the field correlation the problem of finding the perfect pulse could be left completely to the computer.

A major obstacle for the practical implementation of the 1D z-rotation pulse technique for low-field single-sided systems is the time required for resolving different chemical shifts. The lower the field strength, the longer the time, and the current pulse sequences with effective shift evolution during only, say, 5% of the time is clearly not efficient enough. Actually, the 2D nutation sequence with CPMG detection for sensitivity enhancement might prove to be a better choice at low fields and strong gradients. For successful use of the 1D version it is necessary to increase the fraction of the pulse sequence yielding effective chemical shift evolution, and it is possible that this goal could be achieved with optimizations according to the pulse performance criteria presented here.

Although the work presented in this article is only a small step on the way, we foresee that, in the not too distant future, it is possible for non-specialist NMR users, e.g., physicians, industrial engineers, or security personnel, to routinely obtain high-resolution NMR spectra without having to put the sample within an expensive well-shimmed magnet.

Acknowledgments

We thank C.A. Meriles and R.W. Martin for valuable discussions. This work was supported by the Office of Science, Basic Energy Sciences, US Department of Energy under Contract No. DE-AC03-76SF00098. The Swedish Research Council is acknowledged for a postdoctoral fellowship grant (DT).

References

[1] B. Blümich, P. Blümler, G. Eidmann, A. Guthausen, R. Haken, U. Schmitz, K. Saito, G. Zimmer, The NMR-MOUSE: construction, excitation, and applications, Magn. Reson. Imag. 16 (1998) 479–484.

[2] M.D. Hürlimann, D.D. Griffin, Spin dynamics of Carr–Purcell–Meiboom–Gill-like sequences in grossly inhomogeneous B_0 and B_1 fields and application to NMR well logging, J. Magn. Reson. 143 (2000) 120–135.

[3] D.P. Weitekamp, J.R. Garbow, J.B. Murdoch, A. Pines, High-resolution NMR spectra in inhomogeneous magnetic fields: application of total spin coherence transfer echoes, J. Am. Chem. Soc. 103 (1981) 3578–3579.

[4] L.D. Hall, T.J. Norwood, Measurement of high-resolution NMR spectra in an inhomogeneous magnetic field, J. Am. Chem. Soc. 109 (1987) 7579–7581.

[5] S. Vathyam, S. Lee, W.S. Warren, Homogeneous NMR spectra in inhomogeneous fields, Science 272 (1996) 92–96.

[6] Y.-Y. Lin, S. Ahn, N. Murali, W. Brey, C.R. Bowers, W.S. Warren, High-resolution, >1 GHz NMR in unstable magnetic fields, Phys. Rev. Lett. 85 (2000) 3732–3735.

[7] Z. Chen, Z. Chen, J. Zhong, High-resolution NMR spectra in inhomogeneous fields via IDEAL (Intermolecular Dipolar-Interaction Enhanced All Lines) method, J. Am. Chem. Soc. 126 (2004) 446–447.

[8] C.A. Meriles, D. Sakellariou, H. Heise, A.J. Moulé, A. Pines, Approach to high-resolution ex situ NMR spectroscopy, Science 293 (2001) 82–85.

[9] H. Heise, D. Sakellariou, C.A. Meriles, A. Moule, A. Pines, Two-dimensional high-resolution NMR spectra in matched B_0 and B_1 field gradients, J. Magn. Reson. 156 (2002) 146–151.

[10] D. Topgaard, A. Pines, Self-diffusion measurements with chemical shift resolution in inhomogeneous magnetic fields, J. Magn. Reson. 168 (2004) 31–35.

[11] L. Frydman, T. Scherf, A. Lupulescu, The acquisition of multidimensional NMR spectra within a single scan, Proc. Natl. Acad. Sci. USA 99 (2002) 15858–15862.

[12] B. Shapira, A. Lupulescu, Y. Shrot, L. Frydman, Line shape considerations in ultrafast 2D NMR, J. Magn. Reson. 166 (2004) 152–163.

[13] Y. Shrot, L. Frydman, Spatially resolved multidimensional NMR spectroscopy within a single scan, J. Magn. Reson. 167 (2004) 42–48.

[14] B. Shapira, L. Frydman, Spatial encoding and the acquisition of high-resolution NMR spectra in inhomogeneous magnetic fields, J. Am. Chem. Soc. 126 (2004) 7184–7185.

[15] A. Jerschow, Multiple echoes initiated by a single radio frequency pulse in NMR, Chem. Phys. Lett. 296 (1998) 466–470.

[16] A. Scharfenecker, I. Ardelean, R. Kimmich, Diffusion measurements with the aid of nutation spin echoes appearing after two inhomogeneous radiofrequency pulses in inhomogeneous magnetic fields, J. Magn. Reson. 148 (2001) 363–366.

[17] D. Sakellariou, C.A. Meriles, A. Moule, A. Pines, Variable rotation composite pulses for high resolution nuclear magnetic resonance using inhomogeneous magnetic and radiofrequency fields, Chem. Phys. Lett. 363 (2002) 25–33.

[18] C.A. Meriles, D. Sakellariou, A. Pines, Broadband phase modulation by adiabatic pulses, J. Magn. Reson. 164 (2003) 177–181.

[19] D. Sakellariou, C.A. Meriles, A. Pines, Advances in ex situ nuclear magnetic resonance, C. R. Phys. 5 (2004) 337–347.

[20] D. Rosenfeld, S.L. Panfil, Y. Zur, Design of selective adiabatic inversion pulses using the adiabatic condition, J. Magn. Reson. 129 (1997) 115–124.

[21] T.-L. Hwang, P.C.M. van Zijl, M. Garwood, Fast broadband inversion by adiabatic pulses, J. Magn. Reson. 133 (1998) 200–203.

[22] M.A. Smith, H. Hu, A.J. Shaka, Improved broadband inversion performance for NMR in liquids, J. Magn. Reson. 151 (2001) 269–283.

[23] M. Garwood, L. DelaBarre, The return of the frequency sweep: designing adiabatic pulses for contemporary NMR, J. Magn. Reson. 153 (2001) 155–177.

[24] M. Garwood, Y. Ke, Symmetric pulses to induce arbitrary flip angles with compensation for RF inhomogeneity and resonance offsets, J. Magn. Reson. 94 (1991) 511–525.

[25] S. Wimperis, Broadband, narrowband, and passband composite pulses for use in advanced NMR experiments, J. Magn. Reson. A 109 (1994) 221–231.

[26] M.D. Hürlimann, Diffusion and relaxation effects in general stray field NMR experiments, J. Magn. Reson. 148 (2001) 367–378.

[27] D.I. Hoult, R.E. Richards, The signal-to-noise ratio of the nuclear magnetic resonance experiment, J. Magn. Reson. 24 (1976) 71–85.

[28] S. Antonijevic, S. Wimperis, High-resolution NMR spectroscopy in inhomogeneous B_0 and B_1 fields by two-dimensional correlation, Chem. Phys. Lett. 381 (2003) 634–641.

[29] V. Demas, D. Sakellariou, C.A. Meriles, S. Han, J. Reimer, A. Pines, Three-dimensional phase-encoded chemical shift MRI in the presence of inhomogeneous fields, Proc. Natl. Acad. Sci. USA 101 (2004) 8845–8847.

[30] J. Baum, R. Tycko, A. Pines, Broadband and adiabatic inversion of a two-level system by phase-modulated pulses, Phys. Rev. A 32 (1985) 3435–3447.

[31] D. Topgaard, R.W. Martin, D. Sakellariou, C.A. Meriles, A. Pines, "Shim pulses" for NMR spectroscopy and imaging, Proc. Natl. Acad. Sci. USA 101 (2004) 17576–17581.

[32] T.E. Skinner, T.O. Reiss, B. Luy, N. Khaneja, S.J. Glaser, Reducing the duration of broadband excitation pulses using optimal control with limited RF amplitude, J. Magn. Reson. 167 (2004) 68–74.

[33] P.T. Callaghan, Principles of Nuclear Magnetic Resonance Microscopy, Clarendon Press, Oxford, 1991.

[34] R. de Beer, D. van Ormondt, Analysis of NMR data using time domain fitting procedures, NMR: Basic Princ. Progr. 26 (1992) 201–248.

[35] D. Barache, J.-P. Antoine, J.-M. Dereppe, The continuous wavelet transform, an analysis tool for NMR spectroscopy, J. Magn. Reson. 128 (1997) 1–11.

[36] H. Serrai, L. Senhadji, J.D. de Certaines, J.L. Coatrieux, Time-domain quantification of amplitude, chemical shift, apparent relaxation time T_2^*, and phase by wavelet-transform analysis.

Application to biomedical magnetic resonance spectroscopy, J. Magn. Reson. 124 (1997) 20–34.
[37] Y.-Q. Song, L. Venkataramanan, M.D. Hürlimann, M. Flaum, P. Frulla, C. Straley, T_1–T_2 correlation spectra obtained using a fast two-dimensional Laplace inversion, J. Magn. Reson. 154 (2002) 261–268.
[38] P. Stoica, T. Sundin, Exact ML estimation of spectroscopic parameters, J. Magn. Reson. 145 (2000) 108–114.